INVESTIGATION OF PHOTODETECTORS USING GRAPHENE FIELD EFFECT TRANSISTORS IN COMBINATION WITH FUNCTIONAL DYE MATERIALS

A Thesis Submitted to
the Graduate School of Engineering and Sciences of
İzmir Institute of Technology
in Partial Fulfillment of the Requirements for the Degree of

MASTER OF SCIENCE

in Photonics Science and Engineering

by
Ozan YAKAR

July 2020
İZMİR

ACKNOWLEDGMENTS

I would like to express my gratitude to Balcı family for creating a happy and welcoming laboratory and especially to my academic advisor Assoc. Prof. Dr. Sinan Balcı for all he teached me, his wisdom and guidance during my master's degree.

I would also like to thank to my co-supervisor Prof. Dr. Hasan Şahin for his guidance throughout my master's degree, starting from my very first day at IZTECH.

I would like to express my deepest love to my fiancée Elifnur Yazıcı, who always supported and encouraged me with her continuous motivation to help me to work harder.

I would like to thank to my friends, Fehmi Uğur Ünal and Sercan Özen who always loved and supported me during my time at IZTECH.

I would also like to thank to my friends Onur Karaoğlu, Burkay Uzlu, Görkem Özenç, Yekta Kılınçalp and Ozan Güler for their continuous friendship.

Lastly, I would like to thank my family, who helped me become who I am today with their endless love and support.

This reasearch was supported by the TUBITAK with project number 117F172.

ABSTRACT

INVESTIGATION OF PHOTODETECTORS USING GRAPHENE FIELD EFFECT TRANSISTORS IN COMBINATION WITH FUNCTIONAL DYE MATERIALS

A J-aggregate dye is a type of water-soluble, functional dye, which has a sharp and narrow absorption peak after it self-assembles into a brick-wall structure at high concentrations. The absorption peak of the J-aggregates is sharp, narrow and shifted to longer wavelengths compared to their monomer form and it is in the visible or near infrared spectrum. Due to its very sharp and narrow absorption, it has been used in silver halide photography, non-linear optics, lasing and sensing applications. On the other hand, graphene is one atom layer thick, honeycomb lattice of carbon atoms. In the pure, freestanding form, the bands of its electronic structure touch at one point, making it a gapless semimetal. Due to this characteristic, it is possible to manipulate its optical and electronic properties by changing the Fermi energy of graphene. Therefore, graphene found applications in many fields such as light emitting diodes, photodetectors, Hall sensors, optical modulators and flexible optoelectronics.

The functional dye materials have not been combined with graphene photodetectors even though they are highly sensitive to light, less toxic than their competitors and stable at room temperature. In this thesis, using a J-aggregate dye, which has a sharp absorption peak around 585 nm wavelength, a graphene phototransistor has been demonstrated. By changing the charge concentration on graphene, using the charge carriers that arise from the excitation of J-aggregate dye, reversible modulation of graphene Dirac point has been demonstrated. In addition, a novel thin film formation technique has been developed in this study. Porous polyethylene membrane has been used to create thin films of water-soluble materials, such as J-aggregates, on hydrophobic surfaces.

ÖZET

FONKSİYONEL BOYA MALZEMELERİ İLE GRAFİN ALAN ETKİ TRANSİSTÖRLERİ KULLANAN FOTODEDEKTÖRLERİN ARAŞTIRILMASI

J-agrega boya, yüksek yoğunluklarda bir tuğla duvar yapısına kendiliğinden birleştikten sonra keskin ve dar bir soğurma spektrumu tepe noktasına sahip olan, suda çözünür, fonksiyonel bir boya türüdür. J-agregalarının soğurma tepe noktası keskin, dar ve monomer formlarına kıyasla daha uzun dalga boylarına kaymış durumdadır. Bu nokta, görünür veya yakın kızılötesi spektrumda bulunur. Çok keskin ve dar soğurması nedeniyle gümüş halid fotoğrafçılığında, doğrusal olmayan optikte, lazerle ve algılama uygulamalarında kullanıldı. Öte yandan grafin, bir atom tabakası kalınlığında, karbon atomlarından oluşan bal peteği benzeri bir yapıdadır. Saf, bağımsız formda, elektronik yapısının bantları bir noktada dokunarak enerji bant yapısında boşluk bulunmayan bir semimetal oluşturur. Elektronik yapısı nedeniyle, yük taşıyıcı yoğunluğunu değiştirerek grafinin Fermi enerjisini değiştirmek, optik ve elektronik özelliklerini manipüle etmek mümkündür. Grafinin benzersiz özellikleri, ışık yayan diyotlar, fotodetektörler, Hall algılayacıları, optik modülatörler ve esnek optoelektronik gibi birçok alanda uygulama buldu.

Fonksiyonel boya malzemeleri rakiplerinden daha az zehirli olmalarına ve oda koşullarında kararlı olmalarına rağmen grafin ile ortak bir yapıda kullanılmamıştır. Bu tezde, 600 nanometre dalga boyunda keskin bir soğurma spektrumu tepe noktasına sahip olan bir J-agrega boya kullanılarak, bir grafin fototransistörü ve grafinin spektral hassasiyeti arttırılmıştır. Işık kullanılarak grafin üzerindeki yük yoğunluğu değiştirilmiş, enerji bandı yapısındaki Dirac noktasında geri çevrilebilir bir modülasyon gösterilmiştir. Ayrıca, bu çalışmada yeni bir ince film oluşturma tekniği geliştirilmiştir. Gözenekli polietilen membran, hidrofobik yüzeyler üzerinde J-agregaları gibi suda çözünür malzemelerin ince filmlerini oluşturmak için kullanılmıştır.

TABLE OF CONTENTS

LIST OF FIGURES

LIST OF ABBREVIATIONS

FET . . . . . Field Effect Transistor

GFET . . . . . Graphene Field Effect Transistor

CVD . . . . . Chemical Vapor Deposition

TDBC . . . . . 5,5',6,6'-Tetrachlorodi (4-Sulfobutyl) -Benzimidazolocarbocyanine

MC . . . . . Membrane Casting

AOTF . . . . . Acousto Optic Tunable Filter

CHAPTER 1

INTRODUCTION

1.1. Background

Graphene is a one atom layer thick, sp^2 hybridized, single layer carbon lattice that is stable at room conditions. The structure of graphene was predicted by Philip Russell Wallace in 1947.[1] Although, such structure promised unique electrical and optical properties, prior to its discovery, films as thin as graphene were considered to be too unstable.[2] However, its chemical and thermal stability, flexibility and its 2.3% absorption although it is a single atom layer thick material, have attracted a great amount of interest after it is experimentally demonstrated by using the mechanical exfoliation technique from bulk graphite.[2] Due to its energy band structure, its electrical and optical properties are, as predicted, unique. Graphene has been used in many fields, such as light emitting diodes,[3] photodetectors,[4] Hall sensors,[5] lasers,[6] optical modulators,[7] infrared camouflage,[8] solar cells,[9] liquid crystal displays,[10] organic light emitting diodes,[11] flexible optoelectronics.[12] All of such applications are enabled by the variation in charge carrier density on graphene.[13,14]

The number of charge carriers (electrons, holes) per volume is charge carrier concentration or carrier density. The charge carrier concentration on graphene affects directly the electronic and the optical properties of graphene. Consequently, changing the carrier concentration of graphene, doping, is an extensive area of research. There are several ways to change the carrier concentration in graphene. Doping can be done chemically,[15] electrostaticly[16][17] or by photo-induction.[18] For example, the chemical doping uses placing chemical compounds or particles inside or near graphene. While the electrostatic gating is achieved by applying an electric field on graphene layer, which affects the carrier density, photo-induced doping is obtained by placing a light sensitive compound on or near graphene to use the light interaction from compound to transfer charge carriers and change the charge density on graphene.[18][19]

In the photodetection field, photo-induced doping has gained special interest for graphene based devices because of their high photoresponsivity[20] and short response times.[21] Graphene has been previously combined with quantum dots,[22] dipolar chromophores,[18] perovskites,[23] MoS_2,[24] WS_2[25] and yeilded[26] photoresponsivities that are higher than $\sim 10^8 \frac{A}{W}$ with high doping levels $\sim 10^{12} cm^{-2}$. Hence, graphene combined devices show promise in photodetection field. However, there is a whole group of functional dye materials that have not been studied in combination with graphene.

In this thesis, photo-induced doping was studied using a graphene field effect transistor combined with a J-aggregate dye.

Aggregate dyes are self-assembled molecules, which have a very sharp and narrow absorption peak. They self-assemble at high concentrations and depending on one of its two types, upon aggregation, their absorption peak shifts to longer (J-aggregates) or shorter wavelengths (H-aggregates). J-aggregates were discovered in 1936 by Jelley[27] and Scheibe.[28] Since then, they have been used in sensitive and selective detection of molecules,[29] solar cells,[30] polariton lasers,[31] non-linear optical devices,[32] exciton-polaritons[33],[34] syntheses of plexcitonic nanoparticles[35],[36] photodetectors.[37]

Having a very intense and narrow absorption peak in the visible spectrum makes J-aggregates a very good candidate for use in photodetectors. Making use of excitonic properties of J-aggregate dyes,[38] the spectral sensitivity of the graphene has been increased and a new photodetector, using a photo-gated graphene field effect transistor, has been demonstrated. The doping level of graphene was dynamically controlled by using incident photons.

1.2. Electrical Properties of Graphene

The honeycomb-like structure of graphene is formed by hexagonal, monolayer lattice of carbon atoms. The lattice structure is shown in Fig. 1.1(a).

The lattice vectors can be written as,

$$\mathbf{a_1} = \frac{a}{2}(3, \sqrt{3}) \text{ and } \mathbf{a_2} = \frac{a}{2}(3, -\sqrt{3}) \tag{1.1}$$

The graphene lattice, which consists of A and B sublattices, can be defined as lattice vectors $\mathbf{a_1}$ and $\mathbf{a_2}$, where a is the distance between the adjacent carbon atoms and

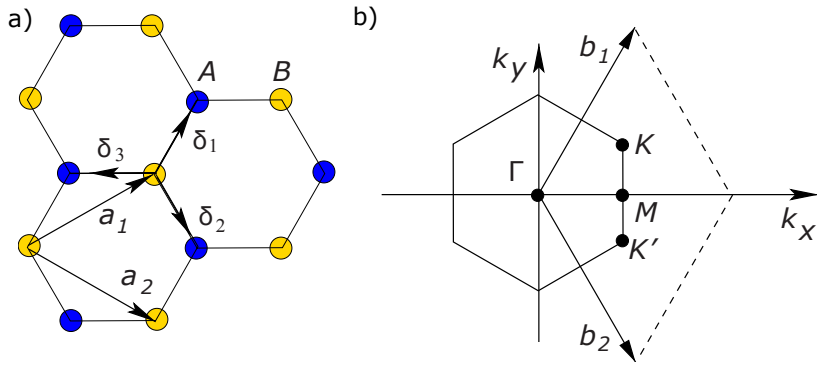

Figure 1.1. (a) Hexagonal honeycomb lattice structure of graphene. (b) Brillouin zone of graphene.[39]

it corresponds to 0.142 nm. The thickness of a single layer graphene is 0.335 nm.

At the Brillouin zone (1.1(b)), the reciprocal lattice vectors can be written as[40]

$$\mathbf{b_1} = \frac{2\pi}{3a}(1, \sqrt{3}),\ \mathbf{b_2} = \frac{2\pi}{3a}(1, -\sqrt{3}) \text{ and } |\mathbf{b_1}| = |\mathbf{b_2}| = \frac{4\pi}{\sqrt{3}a} \tag{1.2}$$

The Brillouin symmetry point vectors K and K' on the Fig. 1.1 (b) are given by vectors[40]

$$\mathbf{K} = (\frac{2\pi}{3a}, \frac{2\pi}{3\sqrt{3}a}),\ \mathbf{K'} = (\frac{2\pi}{3a}, -\frac{2\pi}{3\sqrt{3}a}), \tag{1.3}$$

The nearest neighbor vectors in space are given by,[40]

$$\delta_\mathbf{1} = \frac{a}{2}(1, \sqrt{3}),\ \ \delta_\mathbf{2} = \frac{a}{2}(1, -\sqrt{3}),\ \text{and } \delta_\mathbf{3} = -a(1, 0) \tag{1.4}$$

In the hexagonal lattice structure, carbon atoms are connected to neighboring C atoms by σ bonds in their $2s$, $2p_x$ and $2p_y$ orbitals. The high strength of the graphene structure is due to these bonds.[41] They do not contribute the charge transfer.[39] In addition, the out of plane, $2p_z$, orbital of the carbon atom is free. Since every carbon atom has a free $2p_z$ orbital electron, it can either occupy a spin-up or spin-down state. Moreover, it is not possible for $2p_z$ orbital electron to interact with s or the p_x and p_y orbitals due to the fact they are orthogonal to each other. Therefore, it is possible to treat the $2p_z$ electrons independently in the electronic structure.[42] Hence, the energy levels of σ bonds can be seen separately represented by red dashed lines. Additionally, the $2p_z$ orbitals interact with the neighboring $2p_z$ orbitals and form the π and π^* bands represented by the blue lines in Fig. 1.2(a).

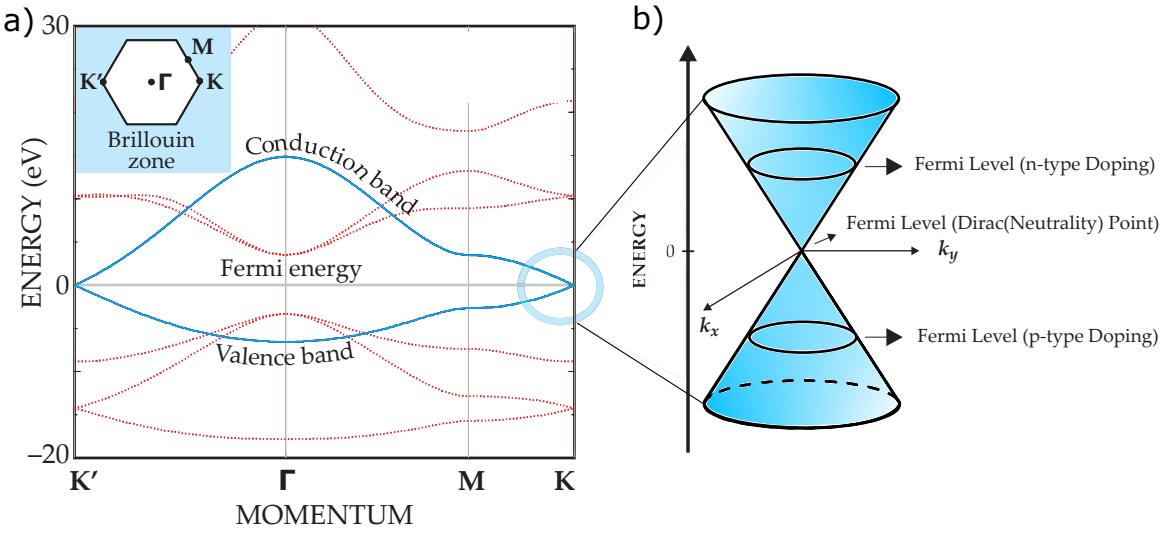

Figure 1.2. (a) Band structure of graphene and (b) schematic representation of the Dirac cone, where E_F is the Fermi energy.[42]

The Brillouin zone symmetry points $K$and K' are of importance to us because the energy varies linearly with the momentum near these points. Therefore, occupied and unoccupied bands touch each other. The point they touch is named the Neutrality (Dirac) point because the number of charge carriers is at its minimum at that point. Therefore, graphene is considered as a gapless semimetal since the valence and conduction bands only touch at this point.[39] The linear variation of energy with respect to momentum at the K and K' symmetry points implies that the charges in graphene, behave as massless Dirac Fermions, and are highly mobile at the neutrality point.[43] In addition, estimated group velocity of charge carriers is $1 \times 10^6 m/s$ at Dirac point.[1] Moreover, in the pure, defectless and freestanding graphene, the Fermi energy is expected to be at the Dirac Point.[43]

Since the energy bands are symmetric around the Dirac point, it can be expected that in pure, freestanding, defect free graphene, the holes and the electrons should have the same properties.[43] Moreover, as shown in Fig. 1.2(b), Fermi level can be at different levels than the Dirac point. This is due to the change in the carrier concentration, doping. Due to presence of adsorbates, impurities or an electric field on graphene, the Fermi energy may shift from the Dirac point. If the Fermi level is at a higher energy than the Dirac point, system is said to be electron doped (n-doped), if the Fermi level is at a lower

energy than the Dirac point, system is said to be hole doped (p-doped).[2]

The Fermi energy is directly proportional to the square root of the carrier density,[40] $E_F \sim \sqrt{n}$. By changing the carrier density, it is possible to tune the Fermi energy. Indeed, the Fermi level affects the electrical and optical properties of graphene. Therefore, many applications of graphene devices use Fermi energy modulation. There are several ways to change the Fermi energy of graphene. For instance, it is possible to use a Field Effect Transistor(FET) to manipulate the Fermi energy.[17] In addition, Fermi energy can be modulated chemically.[15] Moreover, it is possible to change the carrier concentration on the graphene by the incident light using a photo-sensitive material and creating a heterojunction that ensures the charge carrier (electron or hole) transfer.[22] The structure of such device is shown in the Section 1.5.

1.3. Optical Properties of Graphene

Optical properties of graphene arise from its electronic properties. Graphene has broadband absorption of $\sim 2.3\%$ in the visible spectrum (400 nm - 750 nm). The transmittance of the graphene is defined by $T = (1 + \frac{1}{2}\pi\alpha)^{-2}$ for every layer of graphene, where the α, the fine structure constant is[44] $\alpha = e^2/\hbar c \sim 1/137$. Taking into account that graphene is a single atom layer thick material, the optical absorption is quite high.

Due to the zero bandgap structure of graphene, depending on the Fermi level, it is possible for photo-excited electrons to do two types of electronic transitions, interband and intraband, as shown in Fig. 1.3.

Interband transitions are the transitions that take place between valence band and the conduction band. The 2.3% absorption of graphene is mainly due to the interband transitions in the electronic structure.[45] If $2E_F > E_P$ where the E_P is the energy of the photon and E_F is the Fermi Energy, interband transitions are not allowed due to Pauli blocking[46] (Fig. 1.3(b)). For the photons with energy $E_P > 2E_F$, interband transitions are allowed. The amount of blocking can be altered by changing the Fermi energy. Therefore, the optical absorption, that is enabled by interband transitions of the graphene, can be manipulated by changing the Fermi energy.[47]

If a photon with an energy that is less than $2E_F$ interacts with the graphene, interband transitions are blocked. However, intraband transitions are allowed. Intraband

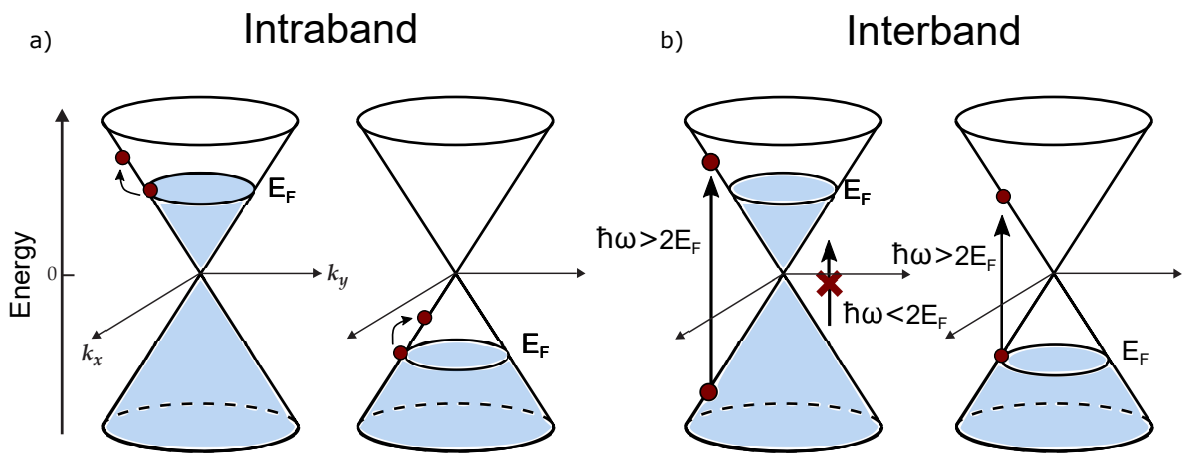

Figure 1.3. Schematic representation of (a) intraband and (b) interband transitions in graphene.

transitions are the transitions within the same band that occur without crossing the Dirac point. Intraband transitions in the graphene are at longer wavelengths and fall into the terahertz part of the electromagnetic spectrum. Moreover, in the terahertz spectrum, graphene behaves similar to a conductive film, and the optical conductivity of graphene is given by the equation, $\sigma(\omega) = \sigma_{DC}(E_F)/(1 + \omega^2\tau^2)$, where $\sigma_{DC}(E_F)$ is the DC electrical conductivity, τ represents the carrier momentum scattering time, ω is the photon frequency. Using this fact, by manipulating the electrical conductivity or Fermi level, the absorption in the terahertz spectrum can also be tuned. Hence, the optical absorption, that is enabled by the interband transitions of graphene, can be modulated by tuning the Fermi energy.[48]

1.4. J-aggregate Dyes

J-aggregate dyes were discovered by Scheibe[28] and Jelley[27] in 1937. They are organic dye molecules that self-assemble at high concentrations. The self-assembly phenomenon is related to the reversible aggregation of the J-aggregate molecules caused by the attractive interaction between the π systems.[4950] The molecular structure of the J-aggregate dye is shown in Fig. 1.4.

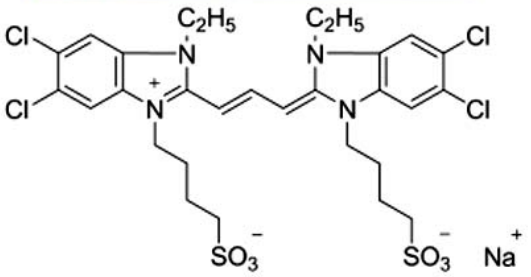

Figure 1.4. Chemical structure of cyanine J-aggregate dye.[35]

Upon aggregation, the absorption peak of aggregated molecules sharpens and shifts to longer or shorter wavelengths (Fig. 1.6). Depending on the shift, they were firstly called J-aggregates, and H-aggregates, respectively.[51] This behavior is correlated with the geometry of the molecular arrangement within the aggregates.[38] The geometry of the aggregates and the delocalization of the electronic states as monomers and dimers are shown in Fig 1.5. In H-aggregates, the geometry of the structure is face to face and the available electronic state is at a higher energy, and thus the absorption peak is seen at shorter wavelengths because the lower energy state transitions are not allowed. On the other hand, in J-aggregates, as shown in the Fig. 1.5(b), the structure is head to tail and the available electronic states in dimer form has a lower energy than the monomer because the higher energy state transitions are not allowed. Therefore, the absorption spectra shift to the longer wavelengths.[52] The modification of the electronic structure is due to the geometric formation of aggregates. The electronic band structure of the aggregates gives rise to excitons. Excitons are a combination of an excited state electron and a hole pair, which are generated upon the excitation. Additionally, the electron and the hole attract each other with electrostatic Coulomb force because of their opposite charges. In the Frenkel exciton theory, the binding energy of the excitons are high. Therefore, they are localized.[53] Moreover, the aggregate dyes are regarded as regular molecular crystals. The dense packing of aggregates gives rise to a strong intermolecular π electronic coupling.[38] Moreover, in the aggregated structure, the monomers are coherently aligned and this enhances the coherent delocalization of the electronic states.[54] Additionally, the electronic excitations in the aggregarates are delocalized over many monomers instead of being confined to a single monomer. In addition, the excited state radiative decay rate is

increased compared to their monomer form.[55] The assembly starts from forming dimers from monomers and then continues on to building the brick wall like structure.

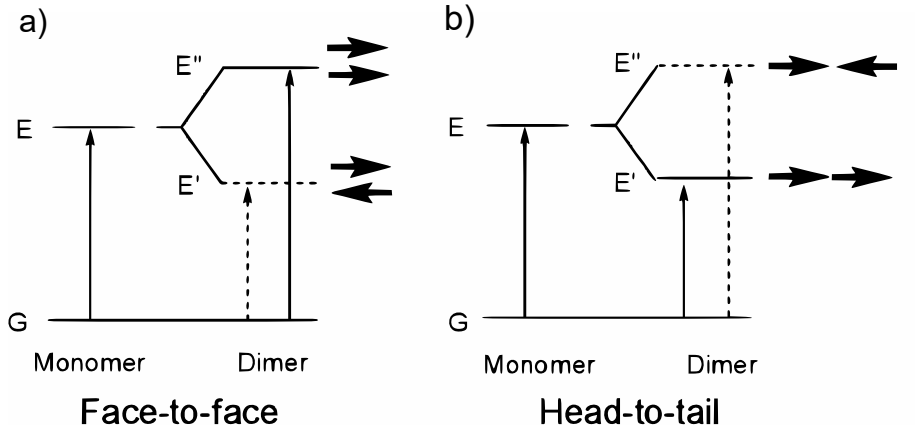

Figure 1.5. The electric band structures for (a) face to face (H-aggregate) and (b) head to tail (J-aggregate) assembled aggregates in monomer and dimer form.[52]

J-aggregates are strong excitonic sources. They are considered to be a model that can efficiently demonstrate a chlorophyll-based light harvesting system.[54]

Non-covalent interactions hold the assemblies of monomers arranged in J-aggregates. The distance between molecules are enough to ignore the electron tunneling effect. Therefore, the properties of energy transfer between molecules and the spectral modifications are due to the Coulomb interactions between the electronic transitions. Molecular aggregates mostly contain their monomer nuclear and electronic structure. Upon aggregation, if the lowest allowed electronic transitions are inside the visible spectrum and the molecules have a big fluorescence and absorption overlap (Fig. 1.6), the electronic transitions become strong enough to transfer to neighboring molecules via de-excitation & excitation process. In this process, an excited electron drops down to the ground state and the generated energy is transferred to the neighboring atom by exciting it. Since the electrons are not mobile in the J-aggregate structures, this transfer occurs via the holes. While the electrons are trapped inside the J-aggregates, the holes can move through.[51] These mobile holes can be used to manipulate the charge carrier concentration on heterojunctions.

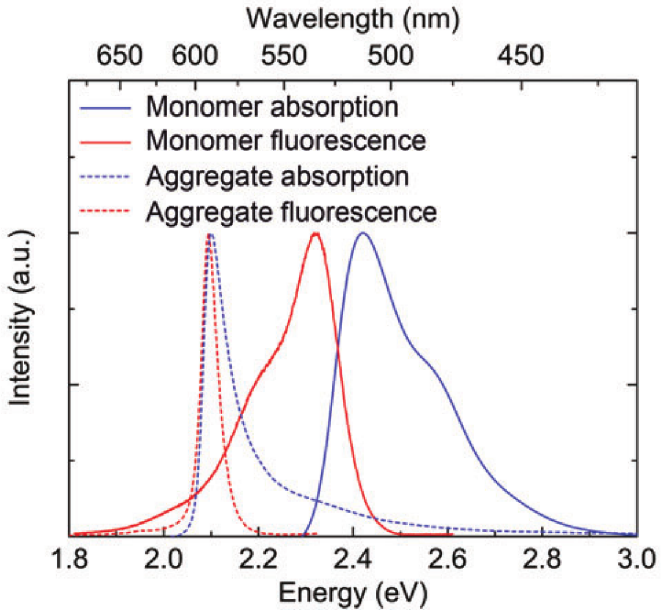

Figure 1.6. Absorption and fluorescence spectra of J-aggregate dye for monomer and aggregate formation in solution.[51]

1.5. Charge Density Modulation on Graphene

One of the ways to modulate the carrier density on the graphene is to use Field Effect Transistors(FET). FET is a device with at least three terminals. The conductivity between two terminals, source-drain, is modulated by the electric field created by the gate terminal.[56] The structures of the top and back-gated FETs are shown in Fig 1.7.

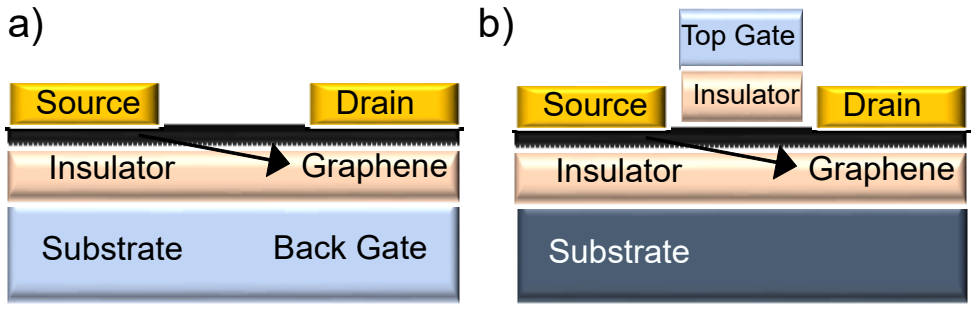

Figure 1.7. Schematic represenatations of (a) back and (b) top gated Graphene Field Effect Transistors

Combined with graphene, this technique was first used in 2004 by Novoselov.[2] The gate voltage manipulates the carrier density on the graphene surface by applying an

electric field on graphene.[57] Therefore, it is possible to use FETs to induce charge carriers and determine the Dirac point of graphene.

Near the Dirac point, the resistivity of the graphene reaches its maximum and in relation, the conductivity reaches its minimum, because the carrier density is at its lowest level.[1] Moreover, at the Dirac point, the density of states vanish.[58] Dirac point can be reached at different gate voltages depending on the purity of the graphene. In defect free, pure, freestanding graphene, the Dirac point is expected to be at zero gate voltage and at zero Fermi level. In the Figure 1.8, Dirac point of a high quality, near doping free graphene is shown.

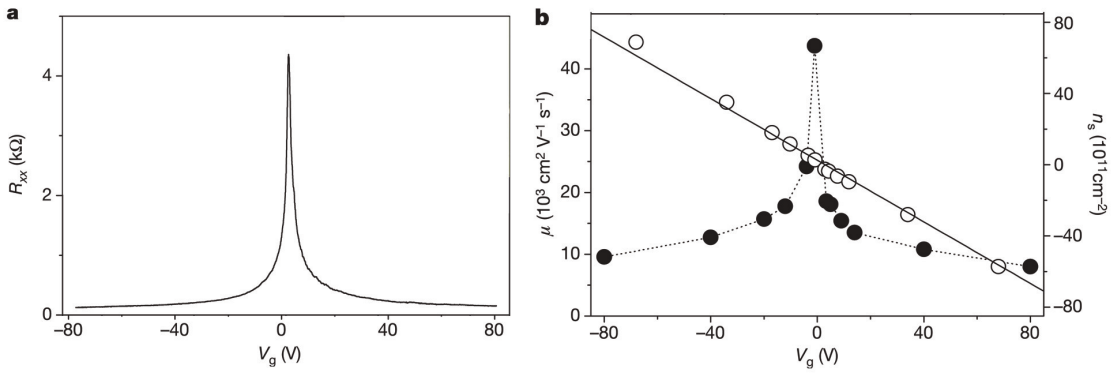

Figure 1.8. (a) Resistivity, (b) mobility (black circles) and carrier concentration (white circles) measurements for varying gate voltages.[58]

Dirac point is measured by scanning the resistance versus the gate voltages and determining the peak. At Dirac point, the resistivity is maximum due to the fact that the density of states vanish and there are no charge carriers. Therefore, it is reasonable to see the resistance peak close to 0 Volt gate voltage in Fig. 1.8(a) since theoretically in pure, free standing graphene, the Dirac point is at 0 Volt.[1] Mobility and charge density measurements are shown in Fig 1.8(b). Around 0 Volt gate voltage, the charge carrier density (white circles) is also at its lowest. Since the effective mass of the electrons are zero at the Dirac point, the mobility of the electrons (black circles) are at their highest.[58]

If the GFETs (Graphene Field Effect Transistors) are combined with a light sensitive material, it is also possible to shift the Dirac point of graphene reversibly using incident light. This, photo-doping, was demonstrated using quantum dots,[59] h-BN,[26] GaN,[60] and perovskites.[61] Depending on the material and the heterojunction, electrons or holes move to the graphene and change the Fermi energy. Since excitons are attracted to each other due to Coulomb interactions, holes tend to move to the highest point of the valence band, and the excited electrons tend to move to the lowest point of the conduction band.[62] The schematic representation of such transfer is shown in the Fig. 1.9. Upon charge carrier transfer, because of the increase or decrease in charge carrier density, the Dirac point of graphene shifts to higher or lower gate voltages for hole transfer or electron transfer, respectively. Therefore, as the gate voltage is scanned versus the resistivity, the peak, at which the Dirac point is measured (Fig. 1.8(a)), shifts to different gate voltages as the charge carrier density on the graphene changes.

In addition to the GFETs, shifting the Dirac point and changing the charge carrier density on graphene, using incident light, is possible by combining a GFET with a light sensitive material. Upon illumination, the charge carriers of the excited photoactive material move to graphene layer. Transferred charge carriers change the population of the charge carriers on graphene and affect the current flowing through the phototransistor.[22]

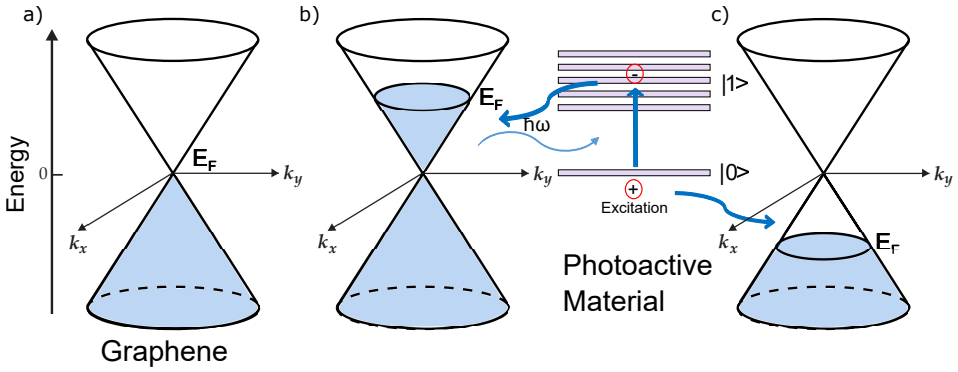

Figure 1.9. Schematic representation of Fermi Energy of graphene (a) before any interaction, after the incident light excites the photoactive material and electrons (b) and holes (c) move to graphene layer and changes its Fermi energy.

Figure 1.9(a) depicts the energy dispersion relation of doping free graphene. When graphene is combined with a photoactive material, upon excitation of the material, elec-

trons move to a higher energy level. Therefore, excited state electrons and holes are created. Depending on the heterostructure, electrons or holes transfer to graphene layer and increase (Fig. 1.9(b)) or decrease (Fig. 1.9(c)) the Fermi level on the graphene, respectively. The change in Fermi energy, therefore in the density of charge carriers, varies the current flowing through the source and drain terminal of the phototransistor. As the charge carriers decrease, the current flowing through the source and drain terminals of the phototransistor decreases, as they increase, the current flowing through the source and drain terminals increases.

J-aggregate dyes can be used as an excitonic source to harvest charge carriers and increase the spectral sensitivity of graphene. When incident photons interact with the J-aggregate dye, an electron-hole pair (exciton) is generated. Although the electrons are trapped inside the J-aggregate and cannot move, the holes in the excited J-aggregate molecules are mobile and can be used to change the charge carrier concentration in Van der Waals (vdW) heterostructures. This gives us a chance to build an all carbon phototransistor, which has been gated by visible light. The holes, that are created upon excitation, are transferred to the graphene layer and lower the Fermi energy of graphene (Fig. 1.9(c)). After hole transfer, the Dirac point is seen at higher gate voltages and going back to the dark condition, it shifts back to its original position. Therefore, the charge density of graphene is reversibly tuned by incident photons.

CHAPTER 2

EXPERIMENTAL METHODS

2.1. Sample Preparation

2.1.1. Synthesis and Transfer of Graphene

Chemical Vapor Deposition (CVD) method has been used in the growth of the graphene. In the CVD method, CH_4 has been used as a carbon supply. Ultrasmooth copper foil (Mitsui Mining and Smelting Company, Ltd, B1-SBS) with $0.1\mu m$ surface roughness was cut into 2 x 2 cm^2 pieces and placed into the tube furnace on top of a quartz glass crystal substrate. Afterwards, the tube was placed under vacuum around ~ 10 mTorrs. After vacuum, under $100sccm$ H_2 flow, the furnace was heated to 1035°C and $10sccm$ CH_4 for 60 seconds. Later, hydrogen was used in order to remove the oxide layer on the surface of copper foils. At high temperatures, C atoms were separated from the H atoms and form a hexagonal carbon lattice on the copper foils. Then the furnace was cooled down to room temperature naturally while it was kept under vacuum and H_2 flow. Subsequently, vacuum was refilled and the samples were removed from the furnace.

In order to transfer the graphene, a polymer layer was used. The samples were coated with photoresist (Shipley 1813) and left inside a 65°C oven overnight. Afterwards, the photoresist was solidified with graphene and copper on one side of it. Next, the copper was etched away using $1M$ $FeCl_3$ solution, and we were left with photoresist and graphene ready to transfer onto a surface. In this case, silicon wafer, which was coated with 300 nm Si_3N_4 was used. To transfer, graphene-polymer layer was placed on a dielectric substrate, which was cut into pieces ($2x3cm^2$) and was heated up to $80C$ for three minutes and then to 110°C for one minute. After letting it cool down to room temperature; acetone, isopropyl alcohol and deionized water were used to remove the

polymer layer.

2.1.2. Membrane Casting

There are several ways to create a light sensitive gain medium and graphene heterostructures via placing molecules and materials on graphene. For example, drop casting, supramolecular $\pi - \pi$ stacking,[19] spin coating,[63] drop casting, and layer by layer methods are a few good examples.[64] Since the polymer transferred single layer CVD graphene shows hydrophobic properties, the adhesion on graphene is not enough to create the excitonic thin film on the graphene layer. In this thesis, a new technique[65] has been developed.

As the excitonic source, a cyanine dye J-aggregate, 5,5',6,6'-tetrachlorodi (4-sulfobutyl)-benzimidazolocarbocyanine (TDBC) was used (from FEW chemicals). An aqueous solution of 10 mM of TDBC was prepared. TDBC was used without further purification. The chemical structure of the J-aggregate dye is shown in 1.4.

In order to distribute the cyanine dye evenly on the sample, Membrane Casting (MC) method was used. In this method, porous polyethylene membrane was used to squeeze the J-aggregate dye between the graphene and the membrane (Gelon LIP group, Celgard 2730). The membrane has a $20\mu m$ of thickness and porosity of 40 percent.[66] After $50\mu L$ of TDBC was dropped on the substrate, the porous polyethylene membrane was placed on both the substrate and the dye. The area of the dye is dictated by the size of the polyethylene membrane. Since the polyethylene membrane is highly hydrophobic, the J-aggregate dye cannot penetrate through the membrane. After leaving it in the room conditions for 10 minutes, the water molecules evaporate through the pores of the membrane and as it can be seen from the Figure 2.1, after the membrane was lifted gently, we were left with a film of J-aggregate molecules on the substrate. The optical images of the surfaces show that the formation of the J-aggregate thin film was fairly uniform.

2.1.3. Hybrid Graphene J-aggregate Phototransistor

The device structure is a back-gated graphene field effect transistor. As a photoactive material, a J-aggregate dye was used.

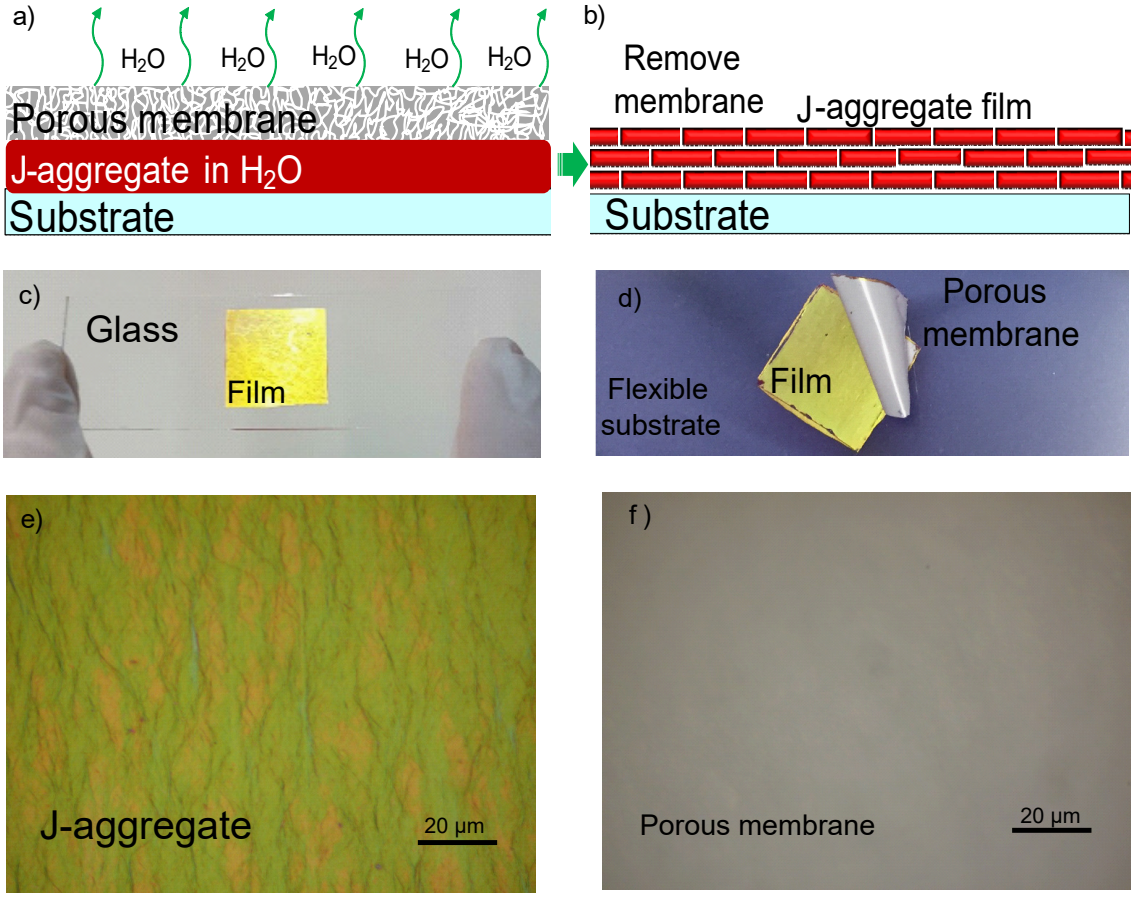

Figure 2.1. (a,b) Schematic representation of Membrane casting technique. (c,d) J-aggregate thin film on glass and flexible substrate, respectively. (e,f) Optical images of J-aggregate thin film and porous membrane.[65]

After graphene was transferred onto the 300 nm silicon nitride coated silicon substrate as mentioned in the Section 2.1.1, the gold electrodes were put into place by thermal evaporation technique. The J-aggregate thin film put on the graphene by membrane casting method mentioned in Section 2.1.2. The final hybrid structure was shown in Fig. 2.2.

The active area of the device is the part that is covered with graphene and J-aggregate dye shown by light red in Fig. 2.2.

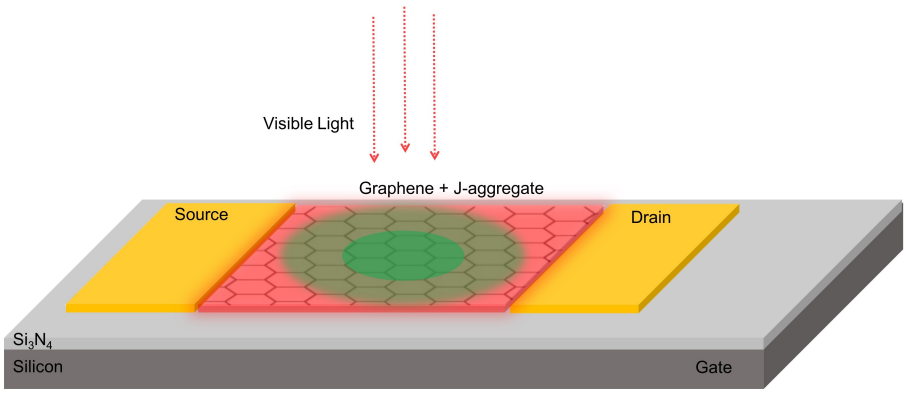

Figure 2.2. Schematic representation of hybrid graphene J-aggregate phototransistor.[65]

2.2. Characterization and Measurement

2.2.1. Raman Spectroscopy

Raman spectroscopy is a tool, which measures the vibrational characteristics in a sample. It was first observed by Sir Ventaka Raman in 1928.[67] The basic principle of Raman spectroscopy is that it compares the energy of the incident light versus the scattered light. When a photon collides with an atom, the electromagnetic field of the photon induces oscillating dipoles in the molecule and therefore, the electromagnetic radiation is produced.

There are three possible outcomes in scattering. First one is Rayleigh scattering, in which the energy of the incident photon is equal to the energy of generated photon. The second and third are called Stokes and anti-Stokes Raman scattering, in which the energy of the scattered photon is lower or higher than the incident photon, respectively (Figure 2.3). Most of the scattering is dominantly Rayleigh. All of these processes include a photon that is absorbed by bringing an atom from the ground state to a virtual state. Then, a new photon is emitted by a transition to the ground state as shown in the Figure 2.3. The energy differences seen in Anti-Stokes and Stokes Raman scattering energies are due to the vibrational characteristics of the sample.[68] The Raman bands are observed when the molecular vibration of the sample causes a change in the polarizability and enables us to distinguish between the structures that emit specific Raman signals.

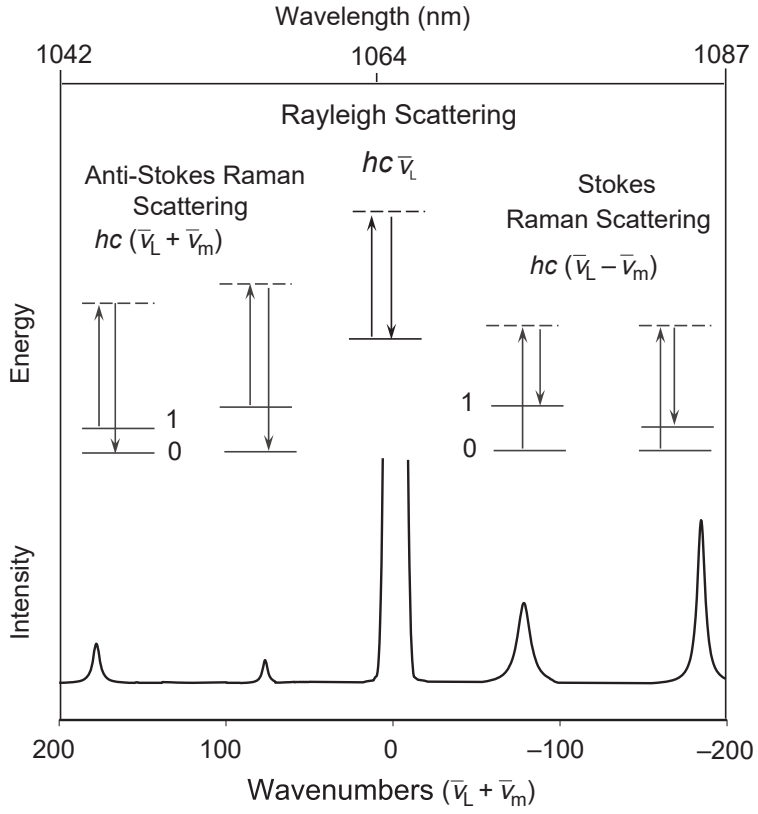

Figure 2.3. Schematic representation of Rayleigh and Raman (Stokes&Anti-Stokes) scattering energies and corresponding wavenumbers.[68]

A Horiba Xplora Plus Raman Microscope is used in the Raman measurements. The system has a Synergicitiy grating spectrometer. For the excitation, 532 nm and 785 nm wavelength lasers were used. The sample is controlled using a motorized XYZ stage.

2.2.2. Profilometer

Profilometer is a device that measures the properties of a surface such as thickness, roughness, etc. There are several types of profilers depending on the methods that they use to determine the characteristics of the surface. These include optical based methods; vertical scanning interferometry, phase shifting interferometry, and contact based methods, stylus profilometer, atomic force microscopy and scanning tunneling microscopy.

Dektak XT was used to measure the thickness of the J-aggregate thin films. Dektak XT is a stylus surface profiler. It keeps its stylus stationary and by moving the sample using a motorized X-Y stage and measuring the deflection of the stylus, and hence it de-

termines the thickness of the material. It is also capable of 3d topological imaging and able to scan in heights ranging from 1 mm down to 5 nm. The vertical resolution of the device is very large and it can be as small as around 0.1 nm.

2.2.3. Absorption and Emission Spectroscopy

Absorption spectroscopy is done by sending a light through a sample and analyzing the characteristics of the transmitted light by putting it through a spectrometer. The absorption characteristics of a sample can be identified using this method.

Emission spectroscopy is based on excitation of molecules into higher energy state by sending a light through a sample, after excitation, excited state electrons falls back to the ground state and emit light. The energy of the emitted photons is analyzed by putting them through a spectrometer. The emission characteristics of a sample can be identified using this method.

Absorption and emission spectroscopy was done by using an Ocean Optics spectrometer. HR4000CG-UV-NIR spectrometer has a linear silicon CCD array as a detector that works in the range of 190 nm to 1100 nm. The spectroscopic range of the spectrometer is between 200 nm and 1100 nm. The optical resolution of the spectrometer is less than 1.0 nm at full width at half maximum.

2.2.4. Electrical and Optical Response Measurements

For the first part of electrical measurements, gate and drain contacts of the phototransistor were connected to a Keithley sourcemeter while the source and drain contacts were connected to another Keithley sourcemeter. Source and gate voltages were supplied from the sourcemeters while current measurements were collected from the same contacts via LabVIEW (Fig. 2.4). Gate voltage is responsible for the electric field on the graphene. On the other hand, the source current flows between the source and drain terminals. For illumination, in order to see the spectral response on different wavelengths, Koheras Versa Supercontunium Laser combined with Acousto Optic Tunable Filter (AOTF) were used. The laser operates between the wavelengths of 400 nm and 2400 nm and has a total output

of 1.5 Watt as a broadband source. It has a spectral width of 1 nm. In order to illuminate the whole area of the phototransistor, the laser beam was expanded and the collimated. After passing through AOTF, the power distribution of the laser at 600 nm wavelength and the spectral distribution of the tunable laser at %50 power were shown in Fig 2.6. At 600 nm wavelength and 100 percent power, the power of the laser is $165 \frac{mW}{cm^2}$.

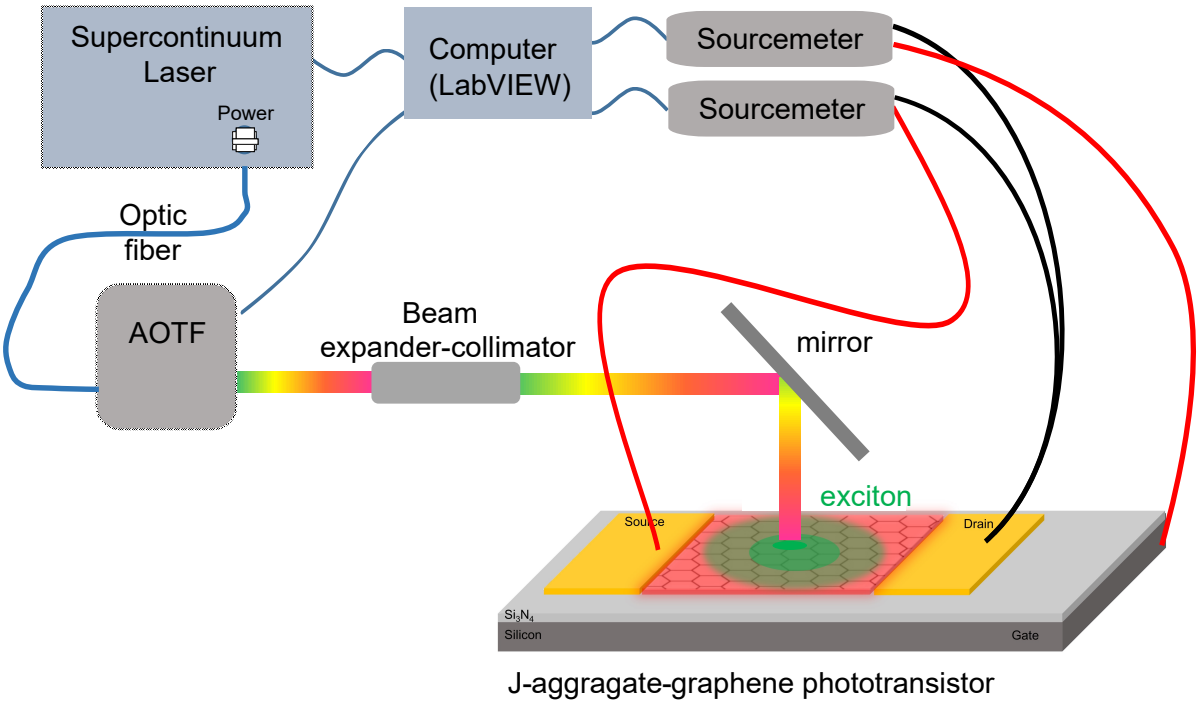

Figure 2.4. Schematic representation measurement setup with tunable wavelength laser.

For the second part of the measurements, the contacts were connected as same as the first part. However, this time the phototransistor was illuminated by a white light (Thorlabs MCWHL5-C Collimated LED). The spectrum of the LED and the schematic representation of the illumination using the white light can be seen from the Fig. 2.5. In addition, the total beam power is 440mW.

Fig 2.6(a) shows that the power of the laser increases linearly with the power control percentage on the laser. Also, the spectral distribution of the laser shows that the output of the laser a 600 nm was suitable for using in our phototransistor measurement (Fig 2.6(b)). Note that these power measurements were done after expanding and collimating the laser beam in order to illuminate the whole surface area.

Using LabVIEW, the wavelength of the incident light was scanned versus the gate

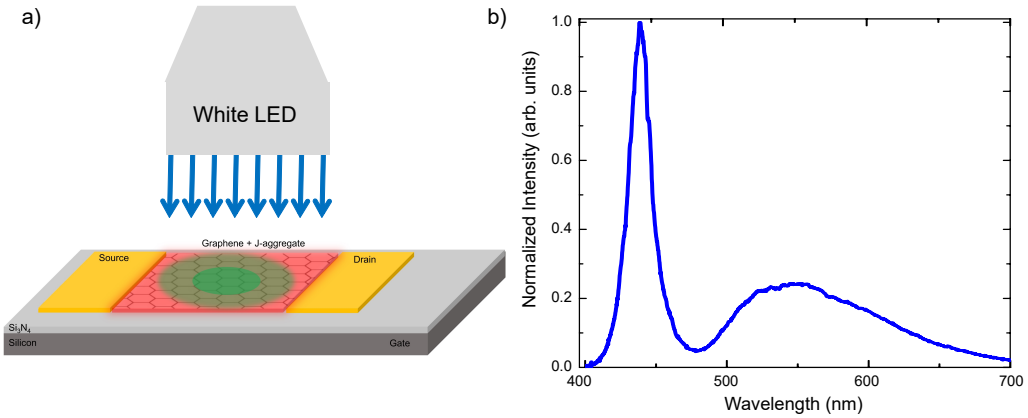

Figure 2.5. (a) Schematic representation of white light illuminated hybrid graphene J-aggregate phototransistor. (b) Spectral distribution of white light.[65]

voltages in the dark and bright conditions, respectively, whereas the current measurements were collected from the sourcemeters via LabVIEW. All the measurements have been done in ambient condition at room temperature.

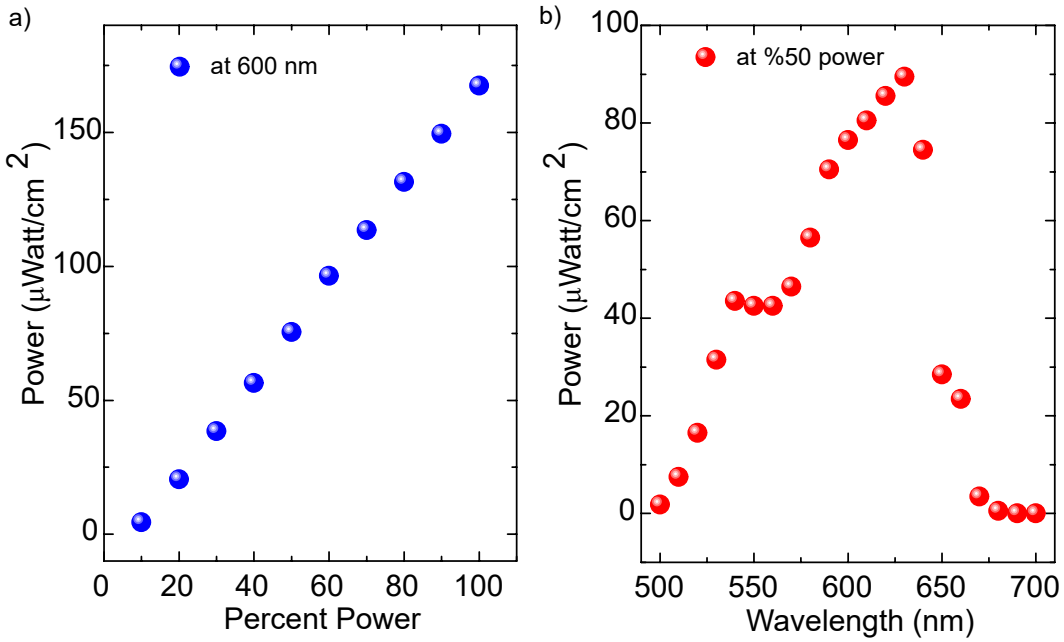

Figure 2.6. (a) Power response of Koheras Versa Supercontiniuum Laser equipped with an Acousto Optic Tunable Filter at 600 nm wavelength. (b) Spectral power distribution of the Koheras Versa Supercontiniuum Laser at %50 power.[65]

CHAPTER 3

RESULTS AND DISCUSSIONS

The J-aggregate dyes were analyzed by absorption and emission spectroscopy in solution and in film forms. Their absorption spectra can be seen in Fig. 3.1. In the absorption spectra, which is measured in solution, the monomer peak was at the 537 nm. As the monomers aggregate, the absorption spectra make a red-shift to 585 nm, a longer wavelength, and the sharpness of the absorption peak increases. This is a characteristic property of J-aggregates and indicates that the molecules are assembled. In the film form, thickness of the aggregated molecules increases and the absorption widens in the visible spectrum. Additionally, the peak of the absorbance in the spectrum was at $\sim$ 595 nm wavelength.

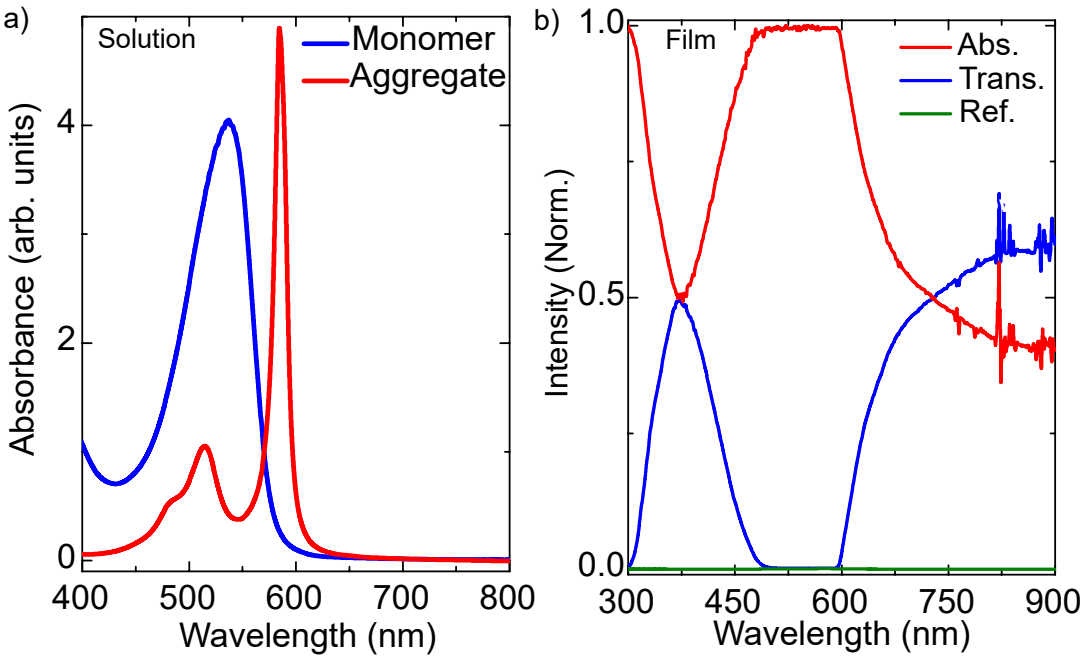

Figure 3.1. (a) Absorption spectra for J-aggregate as monomer and aggregate form in solution. (b) Transmission, absorption spectra for J-aggregate as a thin film.[65]

The narrow and high absorption of the J-aggregate thin film supplies us with a strong excitonic source working in the visible spectrum.

Our CVD graphene was analyzed using Raman spectroscopy on after it was transferred onto a silicon sample.

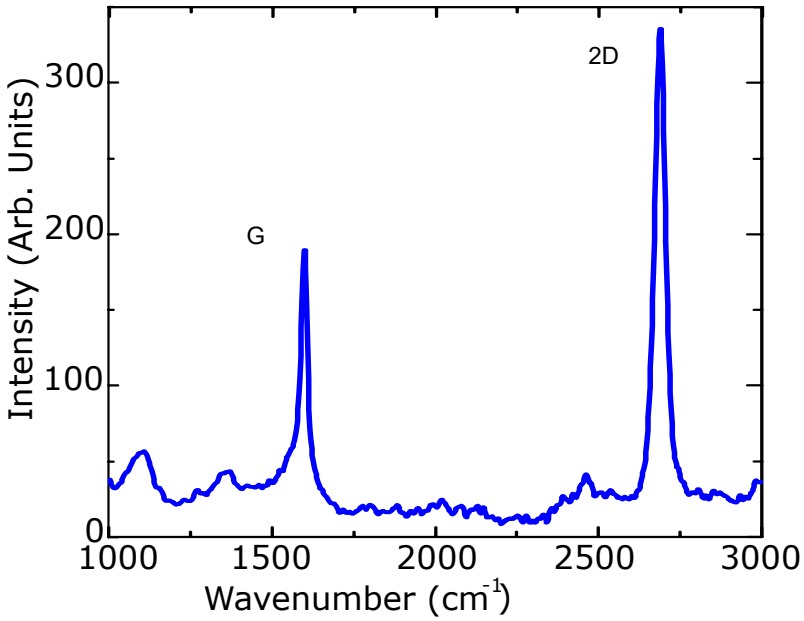

Figure 3.2. Raman spectra for the graphene, which was transferred onto a silicon substrate.[65]

In the Raman spectra, the G peak represents the bond stretching of sp^2 atoms. In addition, the D peak arises from the breathing modes of sp^2 atoms. $2D$ peak in the Raman spectra is the second order of the D peak, which is consisted of half and a quarter of the height of the G peak, $2D_1$ and $2D_2$, respectively.[69] Moreover, the absence of D peak indicates the absence of defects on graphene. As the layers of the graphene increase, the $2D$ peak splits into four components and decreases in the Raman spectra. Additionally, in the single layer graphene, the height of the $2D$ peak is larger than the G peak. As the number of graphene layers increase, the height of the G peak becomes higher than the height of the $2D$ peak. It can be seen from the Raman spectra of the graphene sample (Figure 3.2) that the ratio of G and $2D$ peaks show that the graphene was single layer.[70]

In Fig. 3.3(a), the electrical measurements of the sample show that gate voltage of the Dirac Point was around 40 Volts. In theory, Dirac point of pure, defect free graphene should be at 0 Volt gate voltage.[39] The presence of impurities and adsorbates around the device causes the graphene to be hole doped and lowers its Fermi Energy. Also, the residual transferring polymer also known to hole dope the graphene.[71] All of these factors

cause Fermi energy to decrease and the Dirac point to shift to 40 Volts.

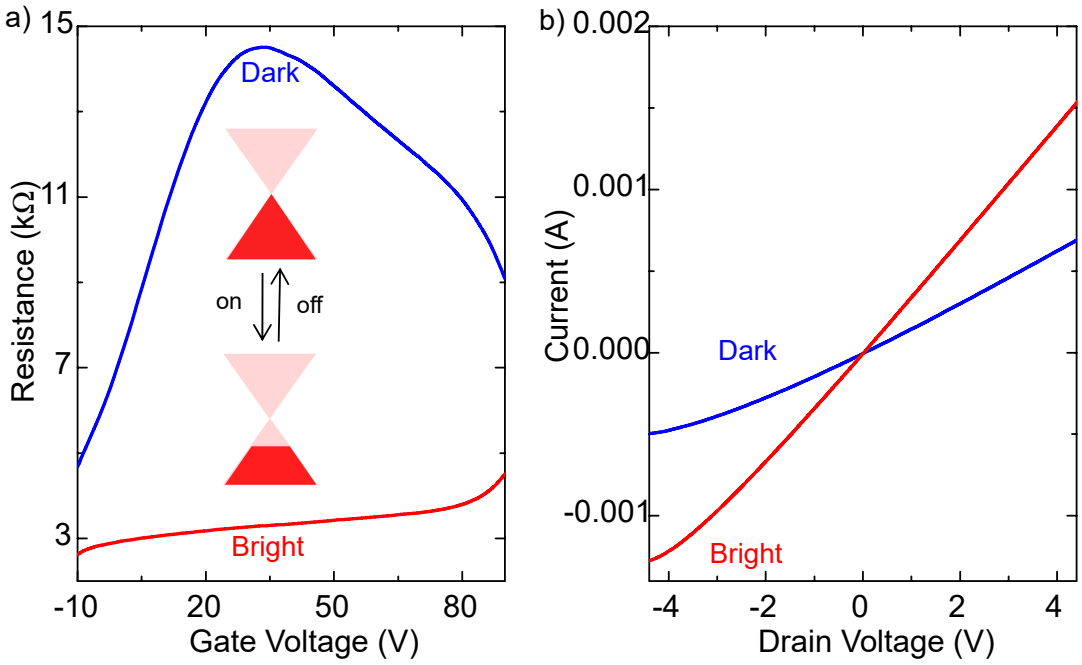

Figure 3.3. (a) Resistance vs. gate voltage measurement for dark and bright conditions. The power of the white light was 440mW. (b) Drain current vs drain voltage in bright and dark conditions where the gate voltage was 0 Volt.[65]

As the light falls onto the device, the incident photons excite the molecule and create electron and hole pairs. Then, the holes are transferred to graphene and make the graphene effectively more hole doped (p doped). The Fermi level of the graphene decreases, therefore, the Dirac point of the graphene is observed at higher gate voltages. However, it was not possible to see exactly where the Dirac Point shifts because going higher than 80 Volts of gate voltages, due to exponentially increasing current between the gate and the drain, leak current, the durability of the insulating material limits us to this interval (Fig. 3.3(a)). Meanwhile, the electrons were trapped inside the J-aggregate molecules, the holes that were transferred into the graphene and drift to the drain and as can be seen from the Fig. 3.3(b), increase the drain current in the bright condition. In this measurement, gate voltage was 0 Volt. The light source that was used to take these measurements was an Olympus broadband white light. The emission spectra of the light source can be seen in Fig. 2.5.

By comparing the resistance values in the dark and bright conditions, it is visible that the Dirac point of the graphene moves to higher gate voltages, reversibly. In order to

see the wavelength specific response, a tunable laser, for which the properties are given in the Section 2.2.4, was used.

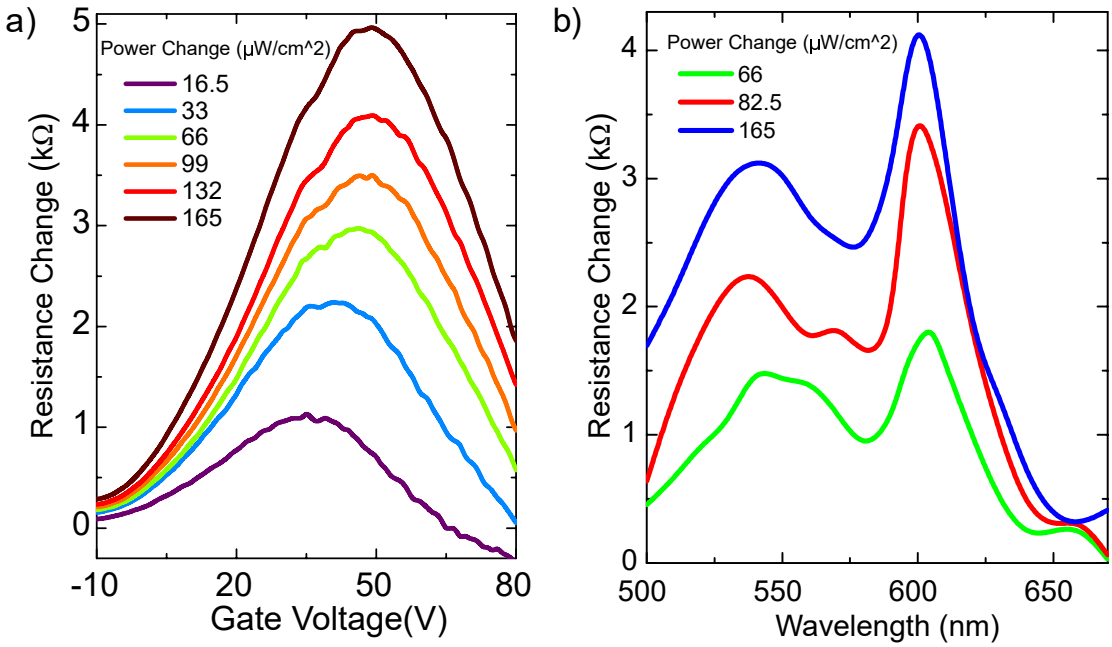

Figure 3.4. (a) Power response of the phototransistor as a function of gate voltage at 600 nm wavelength light and (b) spectral response of the phototransistor at the 40 V gate voltage for varying laser powers.[65]

Photoresponse of the J-aggregate/Graphene transistor as resistance change versus varying gate voltages at 600 nm wavelength incident light as a function of laser power can be seen from the Fig 3.4(a). Most photoresponse as resistance changes was seen at %100 ($165\frac{mW}{cm^2}$) percent laser power. And also, a shift in Dirac point to higher gate voltages was observed as the power of the laser increases. Since, the holes of the excited J-aggregate molecules are transferred to the graphene layer, the Fermi energy of the graphene decreases. Therefore, the Dirac point moves to higher gate voltages.

In order to see the best spectral response of the graphene J-aggregate phototransistor, various wavelengths were scanned. Although, the absorption of the J-aggregate molecules in solution was sharpest at the 585 nm wavelength, in the film formation, the absorption spectra cover most of the visible spectrum. It can be seen from the Fig. 3.4(b), that best spectral response was obtained using 600 nm wavelength light.

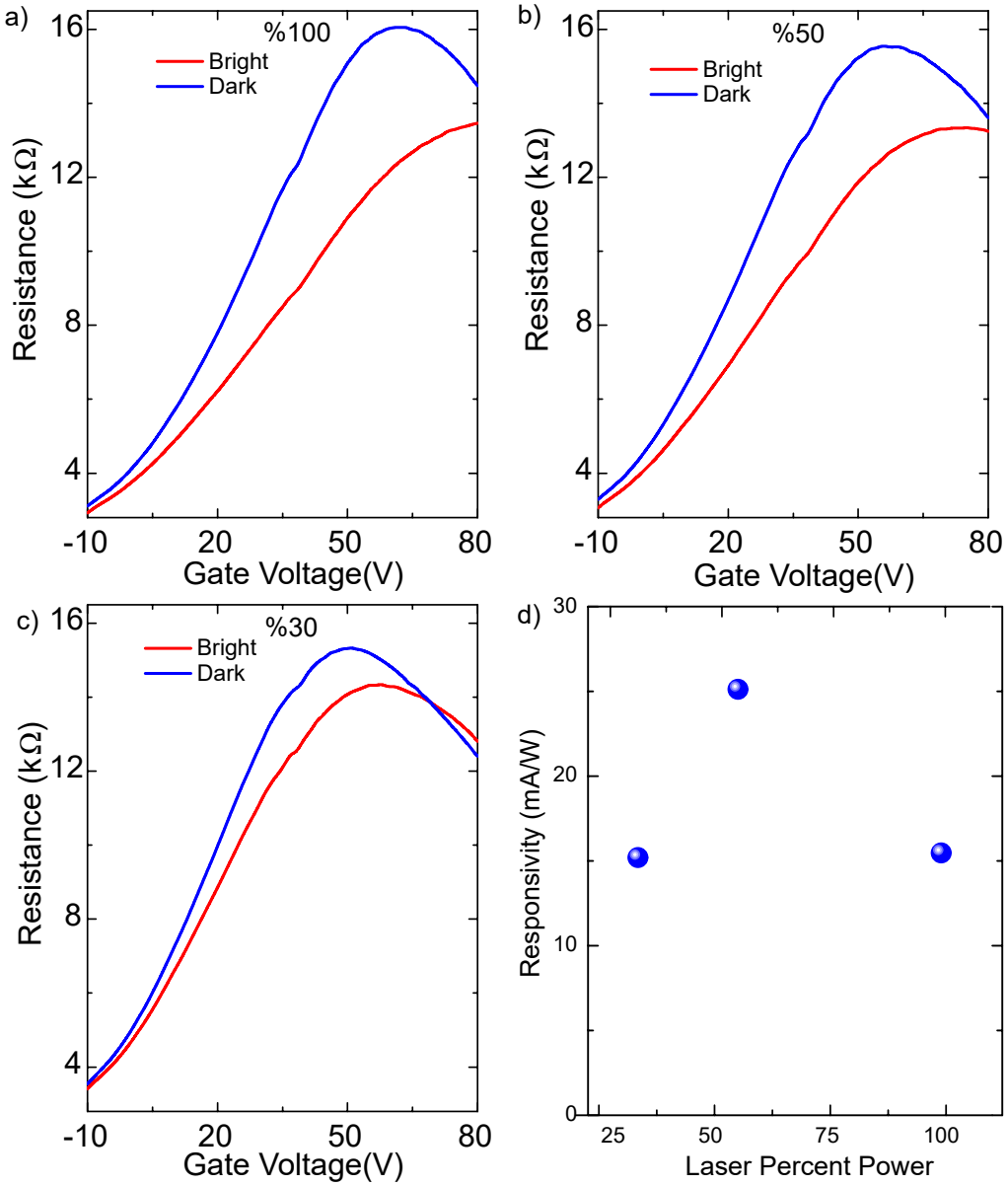

Figure 3.5. Photoresponse of the hybrid graphene-J-aggregate transistor. Resistance change as a function of gate voltage using %100 (a), %50 (b), %30 (c) laser powers at 600 nm wavelength for bright and dark conditions. (d) Calculated photoresponsivity as a function of laser power at 50 Volts gate voltage.[65]

Resistance versus gate voltage measurements for the 600 nm wavelength light of varying powers was shown in the Fig. 3.5. In the bright condition, it can be seen from the results that the holes, that are created due to the excitation of J-aggregate molecules, move to the graphene layer and Dirac point shifts to higher gate voltages due to the decrease in the Fermi energy. The shift in Dirac point is larger at increasing laser powers because the number of photons that excite the J-aggregate molecules is greater. Also, the resistance decreases in the bright condition because the electrons that were trapped inside the J-aggregate dye increase the carrier concentration in the J-aggregate molecules and therefore, the resistivity of the device drops. In the dark condition, since the J-aggregate molecules were not excited, there were no excitons. Therefore, the Fermi level goes back to its original value and the Dirac point was reversibly modulated using incident light.

The performance of a photodetector is measured by its photoresonsivity. Photoresponsivity is the ratio of generated photocurrent to optical power and is given by the following equation,

$$R_P = \frac{\Delta I_P}{P_{laser}} = \frac{I_{bright} - I_{dark}}{P_{laser}} = V_{SD}(\frac{1}{R_{bright}} - \frac{1}{R_{dark}})\frac{1}{P_{laser}} = V_{SD}\frac{R_{dark} - R_{bright}}{R_{dark}R_{bright}P_{laser}}. \tag{3.1}$$

Where the R_P is the photoresponsivity, I_P is the photocurrent, which is determined from the resistance change with constant source drain voltage, V_{SD}, between source and drain terminals, R_{bright} and R_{dark} is the resistance difference in bright and conditions. The photoresponsivity calculations were done by exciting the device at different powers of light, at 40 V gate voltage and 200 mV source-drain voltage. Photoresponsivity of this device was around 26 $\frac{mA}{W}$. Photoresponsivity of the device was low compared to perovskite or quantum dot - graphene hybrid structures. The reason for this is, the area of the device was quite large ($2x2cm^2$) and the impurities in the graphene become more apparent in the electrical measurements as the area increases. Therefore, exploring a similar structure in the micro scale is expected to yield significantly higher photoresponsivities and become comparable with the photoresponsivities of similar structures.

Temporal measurements are done by repeatedly alternating between bright and dark condition. The drops in the Fig 3.6 represents the bright condition. It shows that around 0.5 $k\Omega$ resistance drop occurs in $\sim$ 3 seconds. At higher laser powers, the response was faster as the intensity of the light increases. The rise and fall times of the resistance,

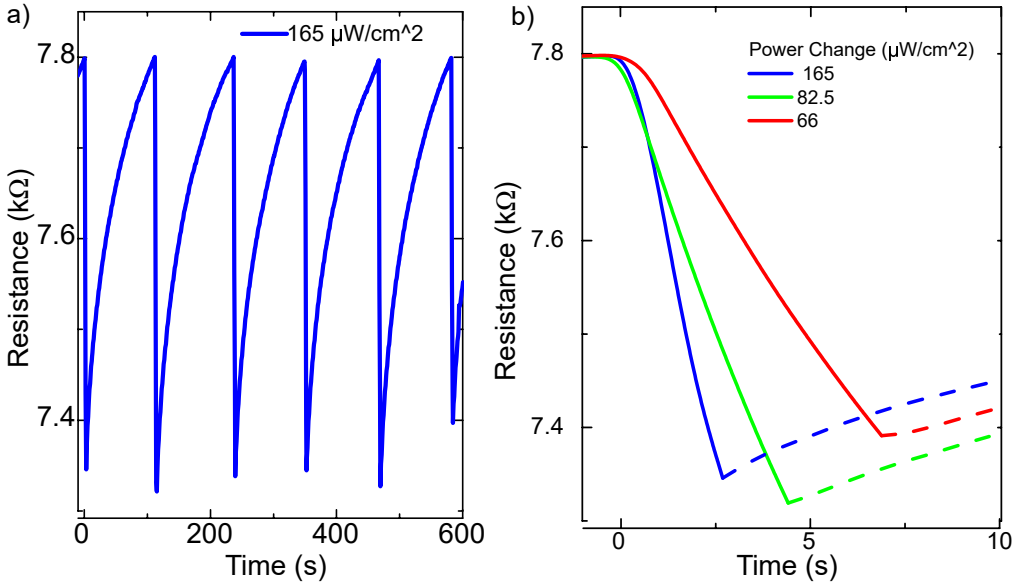

Figure 3.6. Temporal change in resistance, excited by a 600 nm wavelength light with (a) $165\frac{\mu W}{cm^2}$ power and (b) various laser powers.[65]

for bright and dark conditions, are not equal to each other. This can be considered due to the trap states on the surface of graphene-J-aggregate hybrid structures.[72]

CHAPTER 4

CONCLUSIONS

Using graphene, a single layer honeycomb carbon atoms lattice which has charge carriers with effective mass of zero at the Dirac point, a field effect transistor has been demonstrated. Combining graphene field effect transistor with an excitonic dye, J-aggregate, the sharp and narrow absorption peak of J-aggregate in the visible spectrum was used and an all carbon phototransistor has been demonstrated. The Dirac point of graphene has been shifted to higher voltages reversibly via incident photons.

The MC (Membrane Casting) technique was developed. J-aggregate thin films were placed on hydrophobic surfaces, such as polymer transferred graphene, using a porous membrane through which the water molecules can evaporate. Membrane Casting enables us to fabricate thin films of water-soluble materials on hydrophobic surfaces.

Using J-aggregate as a light sensitive material, the spectral sensitivity of graphene has been increased. Furthermore, high absorption of J-aggregate dye in the visible spectrum has been exploited. In addition, the charge carriers of graphene, which act as massless Dirac fermions at the Dirac point of the energy dispersion curve, have been reversibly modulated using incident light. According to the electrical measurements, the graphene was p-doped in its initial form with Dirac point at around 40 Volts. This was due to the adsobates and impurities on the graphene. Residual transfer polymer is known to dope to graphene structure. On the other hand, depending on the power of the light, the Dirac point was shifted higher than 80 volts in less than 3 seconds. This reversible shift, which was created by the incident photons can be used in many graphene based photonics and optoelectronics applications. Moreover, the photoresponsivity of the device was 0.26 $\frac{mA}{W}$. Although the photoresponsivity was low compared to the quantum dot or perovskite combined photodetectors, the smaller devices with similar structures using J-aggregate dyes show promising results that can be comparable to quantum dot or perovskite combined systems. Depending on the J-aggregate dye and the absorption peak, this concept can be used also in different parts of the visible and near infrared spectrum.

REFERENCES

[1] Philip Russell Wallace. The Band Theory of Graphite. *Physical Review*, 71(9):622–634, May 1947.

[2] Konstantin Sergeevich Novoselov, Andre Konstantin Geim, Sergey Morozov, De-eng Jiang, Yi Zhang, Sergey Dubonos, Irina. Grigorieva, and Alexander Firsov. Electric field in atomically thin carbon films. *Science*, 306(5696):666–669, 2004.

[3] Yasuhiro Shirasaki, Geoffrey J. Supran, Moungi G. Bawendi, and Vladimir Bulović. Emergence of colloidal quantum-dot light-emitting technologies. *Nature Photonics*, 7(1):13–23, 2013.

[4] Simone Schuler, Daniel Schall, Daniel Neumaier, Lukas Dobusch, Ole Bethge, Benedikt Schwarz, Michael Krall, and Thomas Mueller. Controlled Generation of a p-n Junction in a Waveguide Integrated Graphene Photodetector. *Nano Letters*, 16(11):7107–7112, 2016.

[5] Burkay Uzlu, Zhenxing Wang, Sebastian Lukas, Martin Otto, Max C. Lemme, and Daniel Neumaier. Gate-tunable graphene-based Hall sensors on flexible substrates with increased sensitivity. *Scientific Reports*, 9(1), 2019.

[6] Han Zhang, Dingyuan Tang, Randy J. Knize, Luming Zhao, Qiaoliang Bao, and Kian Ping Loh. Graphene mode locked, wavelength-tunable, dissipative soliton fiber laser. *Applied Physics Letters*, 96(11):1–4, 2010.

[7] Ming Liu, Xiaobo Yin, Erick Ulin-Avila, Baisong Geng, Thomas Zentgraf, Long Ju, Feng Wang, and Xiang Zhang. A graphene-based broadband optical modulator. *Nature*, 474(7349):64–67, 2011.

[8] Omer Salihoglu, Hasan Burkay Uzlu, Ozan Yakar, Shahnaz Aas, Osman Balci, Nurbek Kakenov, Sinan Balci, Selim Olcum, Sefik Süzer, and Coskun Kocabas. Graphene-Based Adaptive Thermal Camouflage. *Nano Letters*, 18(7):4541–4548, 2018.

[9] Francesco Bonaccorso, Zhipei Sun, Tawfique. Hasan, and Andrea C. Ferrari. Graphene photonics and optoelectronics. *Nature Photonics*, 4(9):611–622, 2010.

[10] Peter Blake, Paul D. Brimicombe, Rahul R. Nair, Tim. Booth, De-en Jiang, Fred Schedin, Leonid A. Ponomarenko, Sergey Morozov, Helen F. Gleeson, Ernie W. Hill, Andre Konstantin Geim, and Konstantin Sergeevich Novoselov. Graphene-based liquid crystal device. *Nano Letters*, 8(6):1704–1708, 2008.

[11] Piotr Matyba, Hisato Yamaguchi, Goki Eda, Manish Chhowalla, Ludvig Edman, and Nathaniel D. Robinson. Graphene and mobile ions: The key to all-plastic, solution-processed light-emitting devices. In *ACS Nano*, volume 4, pages 637–642, 2010.

[12] Emre O. Polat, Osman Balci, Nurbek Kakenov, Hasan Burkay Uzlu, Coskun Kocabas, and Ravinder Dahiya. Synthesis of Large Area Graphene for High Performance in Flexible Optoelectronic Devices. *Scientific Reports*, 5:1–10, 2015.

[13] Anindya Das, Simone Pisana, Biswanath Chakraborty, Stefano Piscanec, Subir Kumar Saha, Umesh V. Waghmare, Konstantin Sergeevich Novoselov, Hulikal Ramaiengar Krishnamurthy, Andre Konstantin Geim, Andrea C. Ferrari, and Ajay K. Sood. Monitoring dopants by Raman scattering in an electrochemically top-gated graphene transistor. *Nature Nanotechnology*, 3(4):210–215, 2008.

[14] Feng Wang, Yuanbo Zhang, Chuanshan Tian, Caglar Girit, Alex Zettl, Michael Crommie, and Y. Ron Shen. Gate-variable optical transitions in graphene. *Science*, 320(5873):206–209, 2008.

[15] Hai I. Wang, Marie Luise Braatz, Nils Richter, Klaas Jan Tielrooij, Zoltan Mics, Hao Lu, Nils Eike Weber, Klaus Müllen, Dmitry Turchinovich, Mathias Kläui, and Mischa Bonn. Reversible Photochemical Control of Doping Levels in Supported Graphene. *Journal of Physical Chemistry C*, 121(7):4083–4091, 2017.

[16] Eduardo J.H. Lee, Kannan Balasubramanian, Ralf Thomas Weitz, Marko Burghard, and Klaus Kern. Contact and edge effects in graphene devices. *Nature Nanotechnology*, 3(8):486–490, 2008.

[17] Amol Singh, Ahsan Uddin, Helene Maire-Afeli, Nick Sbrockey, Gary S. Tompa, Michael G. Spencer, Thomas Vogt, Tangali S. Sudarshan, and Goutam Koley. Electrically tunable molecular doping of graphene. *Applied Physics Letters*, 102(4):10–15, 2013.

[18] Myungwoong Kim, Nathaniel S. Safron, Changshui Huang, Michael S. Arnold, and Padma Gopalan. Light-driven reversible modulation of doping in graphene. *Nano Letters*, 12(1):182–187, 2012.

[19] Piljae Joo, Beom Joon Kim, Eun Kyung Jeon, Jeong Ho Cho, and Byeong Su Kim. Optical switching of the Dirac point in graphene multilayer field-effect transistors functionalized with spiropyran. *Chemical Communications*, 48(89):10978–10980, 2012.

[20] Fang Luo, Mengjian Zhu, Yuan Tan, Honghui Sun, Wei Luo, Gang Peng, Zhihong Zhu, Xue Ao Zhang, and Shiqiao Qin. High responsivity graphene photodetectors from visible to near-infrared by photogating effect. *AIP Advances*, 8(11), 2018.

[21] Krishna Murali, Nithin Abraham, Sarthak Das, Sangeeth Kallatt, and Kausik Majumdar. Highly Sensitive, Fast Graphene Photodetector with Responsivity $>$106 A/W Using a Floating Quantum Well Gate. *ACS Applied Materials and Interfaces*, 11(33):30010–30018, 2019.

[22] Chang Oh Kim, Sung Won Hwang, Sung Kim, Dong Hee Shin, Soo Seok Kang, Jong Min Kim, Chan Wook Jang, Ju Hwan Kim, Kyeong Won Lee, Suk Ho Choi, and Euyheon Hwang. High-performance graphene-quantum-dot photodetectors. *Scientific Reports*, 4:4–9, 2014.

[23] Yuchuan Shao, Ye Liu, Xiaolong Chen, Chen Chen, Ibrahim Sarpkaya, Zhaolai Chen, Yanjun Fang, Jaemin Kong, Kenji Watanabe, Takashi Taniguchi, André Taylor, Jinsong Huang, and Fengnian Xia. Stable Graphene-Two-Dimensional Multiphase Perovskite Heterostructure Phototransistors with High Gain. *Nano Letters*, 17(12):7330–7338, 2017.

[24] Oriol Lopez-Sanchez, Dominik Lembke, Metin Kayci, Aleksandra Radenovic, and Andras Kis. Ultrasensitive photodetectors based on monolayer MoS 2. *Nature Nanotechnology*, 8(7):497–501, 2013.

[25] Liam Britnell, Ricardo Mendes Ribeiro, Axel Eckmann, Rashid Jalil, Branson D. Belle, Artem Mishchenko, Yong Jin Kim, Roman V. Gorbachev, Thanasis Georgiou, Sergey Morozov, Alexander Grigorenko, Andre Konstantin Geim, Cinzia Casiraghi, H. Castro Neto, and Konstantin Sergeevich Novoselov. Strong Light-Matter Interactions Thin Films. *Science*, 340(June):1311–1315, 2013.

[26] Long Ju, Jairo Velasco, Edwin Huang, Salman Kahn, Casey Nosiglia, Hsin Zon Tsai, Wei Yang, Takashi Taniguchi, Katsutoshi Watanabe, Yi Zhang, Guangyu Zhang, Michael Crommie, Alex Zettl, and Fuqiong Wang. Photoinduced doping in heterostructures of graphene and boron nitride. *Nature Nanotechnology*, 9(5):348–352, 2014.

[27] Edwin E. Jelley. Spectral Absorption and Fluorescence of Dyes in the Molecular State. *Nature*, 138(3502):1009–1010, dec 1936.

[28] G. Scheibe. Über die Veränderlichkeit der Absorptionsspektren in Lösungen und die Nebenvalenzen als ihre Ursache. *Angewandte Chemie*, 50(11):212–219, mar 1937.

[29] Weilang Liang, Sihui He, and Jiyu Fang. Self-assembly of J-aggregate nanotubes and their applications for sensing dopamine. *Langmuir*, 30(3):805–811, 2014.

[30] Kazuhiro Sayama, Shingo Tsukagoshi, Kohjiro Hara, Yasuyo Ohga, Akira Shinpou, Yoshimoto Abe, Sadaharu Suga, and Hironori Arakawa. Photoelectrochemical properties of J aggregates of benzothiazole merocyanine dyes on a nanostructured TiO2 film. *Journal of Physical Chemistry B*, 106(6):1363–1371, 2002.

[31] Ioannis Paschos, Nicolo Somaschi, Simeon I. Tsintzos, David Coles, Julia L. Bricks, Zacharias Hatzopoulos, David Lidzey, Pavlos G. Lagoudakis, and Pavlos G. Savvidis. Hybrid organic-inorganic polariton laser. *Scientific Reports*, 7(1):1–7, 2017.

[32] Atsushi Yabushita, Takao Fuji, and Takayoshi Kobayashi. Nonlinear propagation of ultrashort pulses in cyanine dye solution investigated by SHG FROG. *Chemical Physics Letters*, 398(4-6):495–499, 2004.

[33] Hai Wang, Hai Yu Wang, Angelo Bozzola, Andrea Toma, Simone Panaro, Waseem Raja, Alessandro Alabastri, Lei Wang, Qi Dai Chen, Huai Liang Xu, Francesco De Angelis, Hong Bo Sun, and Remo Proietti Zaccaria. Dynamics of Strong Coupling between J-Aggregates and Surface Plasmon Polaritons in Subwavelength Hole Arrays. *Advanced Functional Materials*, 26(34):6198–6205, 2016.

[34] David G. Lidzey, Donal D.C. Bradley, Adam Armitage, Steve Walker, and Maurice S. Skolnick. Photon-mediated hybridization of Frenkel excitons in organic semiconductor microcavities. *Science*, 288(5471):1620–1623, 2000.

[35] Sinan Balci. Ultrastrong plasmon exciton coupling in metal nanoprisms with J-aggregates. *Optics Letters*, 38(21):4498, 2013.

[36] Fadime Mert Balci, Sema Sarisozen, Nahit Polat, and Sinan Balci. Colloidal nanodisk shaped plexcitonic nanoparticles with large rabi splitting energies. *Journal of Physical Chemistry C*, 123(43):26571–26576, 2019.

[37] Brian J. Walker, August Dorn, Vladimir Bulović, and Moungi G. Bawendi. Color-selective photocurrent enhancement in coupled J-aggregate/nanowires formed in solution. *Nano Letters*, 11(7):2655–2659, 2011.

[38] Stefan Kirstein and Helmuth Möhwald. Exciton band structures in 2D aggregates of cyanine dyes. *Advanced Materials*, 7(5):460–463, 1995.

[39] Jean-Christophe Charlier, Peter C. Eklund, Jiaqi Zhu, and Andrea C. Ferrari. Electron and Phonon Properties of Graphene: Their Relationship with Carbon Nanotubes. In *Topics in Applied Physics*, volume 111, pages 673–709. 2007.

[40] Antonio H. Castro Neto, Fransisco Guinea, Nuno Peres, Konstantin Sergeevich Novoselov, and Andre Konstantin Geim. The electronic properties of graphene.

Reviews of Modern Physics, 81(1):109–162, 2009.

[41] Eduardo J.H. Lee, Kannan Balasubramanian, Ralf Thomas Weitz, Marko Burghard, and Klaus Kern. Contact and edge effects in graphene devices. *Nature Nanotechnology*, 3(8):486–490, 2008.

[42] Andre Konstantin Geim and Allan H. MacDonald. Graphene: Exploring carbon flatland. *Physics Today*, 60(8):35–41, 2007.

[43] Phaedon Avouris. Graphene: Electronic and photonic properties and devices. *Nano Letters*, 10(11):4285–4294, 2010.

[44] Rahul R. Nair, Peter Blake, Alexander N. Grigorenko, Konstantin Sergeevich Novoselov, Timothy J. Booth, Tobias Stauber, Nuno Peres, and Andre Konstantin Geim. Fine structure constant defines visual transparency of graphene. *Science*, 320(5881):1308, 2008.

[45] ZhiQuan Li, Erik A. Henriksen, Zhifang Jiang, Zhao Hao, Michael C. Martin, Phaly Kim, Horst Ludwig Stormer, and Dimitri Basov. Dirac charge dynamics in graphene by infrared spectroscopy. *Nature Physics*, 4(7):532–535, 2008.

[46] Wenzhong Bao, Jiayu Wan, Xiaogang Han, Xinghan Cai, Hongli Zhu, Dohun Kim, Dakang Ma, Yunlu Xu, Jeremy Munday, Dennis Drew, Michael S. Fuhrer, and Liangbing Hu. Approaching the limits of transparency and conductivity in graphitic materials through lithium intercalation. *Nature Communications*, 5(1):4224, sep 2014.

[47] Zhipei Sun, Tawfique Hasan, Felice Torrisi, Daniel Popa, Giulia Privitera, Fengqiu Wang, Francesco Bonaccorso, Denis M. Basko, and Andrea C. Ferrari. Graphene mode-locked ultrafast laser. *ACS Nano*, 4(2):803–810, 2010.

[48] Berardi Sensale-Rodriguez, Rusen Yan, Michelle M. Kelly, Tian Fang, Kristof Tahy, Wan Sik Hwang, Debdeep Jena, Lei Liu, and Huili Grace Xing. Broadband graphene terahertz modulators enabled by intraband transitions. *Nature Commu-*

nications, 3:780–787, 2012.

[49] Dietmar Möbius. Scheibe Aggregates. *Advanced Materials*, 7(5):437–444, 1995.

[50] Hans Von Berlepsch, Christoph Böttcher, Andre Quart, Christian Burger, Sven Dähne, and Stefan Kirstein. Supramolecular structures of J-aggregates of carbocyanine dyes in solution. *Journal of Physical Chemistry B*, 104(22):5255–5262, 2000.

[51] Semion K. Saikin, Alexander Eisfeld, Stéphanie Valleau, and Alán Aspuru-Guzik. Photonics meets excitonics: Natural and artificial molecular aggregates. *Nanophotonics*, 2(1):21–38, 2013.

[52] Akiharu Satake and Yoshiaki Kobuke. Artificial photosynthetic systems: Assemblies of slipped cofacial porphyrins and phthalocyanines showing strong electronic coupling. *Organic and Biomolecular Chemistry*, 5(11):1679–1691, 2007.

[53] Roman Schuster, Martin Knupfer, and Helmuth Berger. Exciton Band Structure of Pentacene Molecular Solids: Breakdown of the Frenkel Exciton Model. *Physical Review Letters*, 98(3):037402, jan 2007.

[54] Simanta Kundu and Amitava Patra. Nanoscale strategies for light harvesting. *Chemical Reviews*, 117(2):712–757, 2017.

[55] Frank C. Spano and Carlos Silva. H- and J-Aggregate Behavior in Polymeric Semiconductors. *Annual Review of Physical Chemistry*, 65(1):477–500, 2014.

[56] Dharmendar Reddy, Leonard F. Register, Gary D. Carpenter, and Sanjay K. Banerjee. Erratum: Graphene field-effect transistors (Journal of Physics D: Applied Physics (2011) 44 (313001)). *Journal of Physics D: Applied Physics*, 45(1), 2012.

[57] Jinhua Li, Liyong Niu, Zijian Zheng, and Feng Yan. Photosensitive graphene transistors. *Advanced Materials*, 26(31):5239–5273, 2014.

[58] Yuanbo Zhang, Yan Wen Tan, Horst L. Stormer, and Philip Kim. Experimental ob-

servation of the quantum Hall effect and Berry's phase in graphene. *Nature*, 438(7065):201–204, 2005.

[59] Chang Oh Kim, Sung Won Hwang, Sung Kim, Dong Hee Shin, Soo Seok Kang, Jong Min Kim, Chan Wook Jang, Ju Hwan Kim, Kyeong Won Lee, Suk Ho Choi, and Euyheon Hwang. High-performance graphene-quantum-dot photodetectors. *Scientific Reports*, 4:4–9, 2014.

[60] Tzu Neng Lin, Svette Reina Merden Sandiago Santiago, Chi Tzu Yuan, Ji Lin Shen, Hao Chung Kuo, and Chin Hsin Chiu. Photo-induced Doping in GaN Epilayers with Graphene Quantum Dots. *Scientific Reports*, 6:1–9, 2016.

[61] Yusheng Wang, Yupeng Zhang, Yao Lu, Weidong Xu, Haoran Mu, Caiyun Chen, Hong Qiao, Jingchao Song, Shaojuan Li, Baoquan Sun, Yi Bing Cheng, and Qiaoliang Bao. Hybrid Graphene-Perovskite Phototransistors with Ultrahigh Responsivity and Gain. *Advanced Optical Materials*, 3(10):1389–1396, 2015.

[62] Alexander Govorov, Pedro Ludwig Hernández Martínez, and Hilmi Volkan Demir. Theoretical Approaches: Exciton Theory, Coulomb Interactions and Fluctuation-Dissipation Theorem BT - Understanding and Modeling Förster-type Resonance Energy Transfer (FRET): Introduction to FRET, Vol. 1. pages 41–51. Springer Singapore, Singapore, 2016.

[63] Carlos Redondo-Obispo, Teresa S. Ripolles, Sandra Cortijo-Campos, Angel Luis Álvarez, Esteban Climent-Pascual, Alicia de Andrés, and Carmen Coya. Enhanced stability and efficiency in inverted perovskite solar cells through graphene doping of PEDOT:PSS hole transport layer. *Materials & Design*, 191:108587, jun 2020.

[64] Brendan G. DeLacy, Wenjun Qiu, Marin Soljačić, Chia Wei Hsu, Owen D. Miller, Steven G. Johnson, and John D. Joannopoulos. Layer-by-layer self-assembly of plexcitonic nanoparticles. *Optics Express*, 21(16):19103, 2013.

[65] Ozan Yakar, Osman Balci, Burkay Uzlu, Nahit Polat, Ozan Ari, Ilknur Tunc, Coskun Kocabas, and Sinan Balci. Hybrid J-Aggregate-Graphene Phototransistor. *ACS Ap-*

plied Nano Materials, 3(1):409–417, 2020.

[66] Pankaj Arora and Zhengming Zhang. Battery separators. *Chemical Reviews*, 104(10):4419–4462, 2004.

[67] Chandrasekhara Venkata Raman and Kariamanikkam Srinivasa Krishnan. A New Type of Secondary Radiation. *Nature*, 121(3048):501–502, mar 1928.

[68] Peter Larkin. *Infrared and Raman Spectroscopy; Principles and Spectral Interpretation*, volume 9. Elsevier, 2011.

[69] Andrea C. Ferrari. Raman spectroscopy of graphene and graphite: Disorder, electron-phonon coupling, doping and nonadiabatic effects. *Solid State Communications*, 143(1-2):47–57, 2007.

[70] Andrea C. Ferrari, Jannik C. Meyer, Vittorio Scardaci, Cinzia Casiraghi, Michele Lazzeri, Francesco Mauri, Stefano Piscanec, De-en Jiang, Konstantin Sergeevich Novoselov, Siegmar Roth, and Andre Konstantin Geim. Raman spectrum of graphene and graphene layers. *Physical Review Letters*, 97(18):1–4, 2006.

[71] Onejae Sul, Kyumin Kim, Eunseok Choi, Joonpyo Kil, Wanjun Park, and Seung Beck Lee. Reduction of hole doping of chemical vapor deposition grown graphene by photoresist selection and thermal treatment. *Nanotechnology*, 27(50), 2016.

[72] Gerasimos Konstantatos, Larissa Levina, Armin Fischer, and Edward H. Sargent. Engineering the temporal response of photoconductive photodetectors via selective introduction of surface trap states. *Nano Letters*, 8(5):1446–1450, 2008.